



Off-board electric vehicle battery charger using fuel cell and PV array

Gajjela.kasthuri¹, Dr.Vishwanatha siddharatha²

2281

¹M TECH, Department of Electrical and Electronics Engineering, Cvr College of Engineering, Vastunagar, Mangalpalli (V), Ibrahimpatnam (M), R.R District-510 510, Telangana, India

²Assistant professor, Department of Electrical and Electronics Engineering, Cvr College of Engineering, Vastunagar, Mangalpalli (V), Ibrahimpatnam (M), R.R District-510 510, Telangana, India

email:¹gkasthuri79@gmail.com,²vsiddhu251@gmail.com

Abstract: The usage of renewable energy has dramatically increased over the past few years in a variety of industries, which has led to its use for EV (electric vehicle) battery charging in the automotive sector. In this research, a bidirectional interleaved DC-DC converter (BIDC)-fed off-board battery charging system using photovoltaic (PV) arrays is suggested for light-weight EVs. This off-board charging system has the ability to operate in dual mode, providing power to the EV battery from the PV array when the vehicle is at a standstill and driving the DC load when the vehicle is moving. A three-phase BIDC is used to carry out this dual mode operation. Software called MATLAB/Simulink is used to simulate the suggested system's model. This study provides simulation findings. To increase the system's capacity and reliability of power in shaded conditions, a fuel cell is also connected to the existing system. Simulink from the MATLAB programme is used to simulate the suggested charging mechanism.

Key terms: Solar array, EV, fuel cell, battery, sepic converter and bidirectional DC-DC charger.

1. INTRODUCTION

The ecosystem has suffered due to the ever-increasing strain on fossil fuels, which has also caused the depletion of non-renewable energy sources. This makes clean, plentiful renewable energy sources even more necessary. Solar and wind energy are the two most popular renewable energy sources currently on the market. With the development of technology, these energy sources

were harnessed to transform energy into electricity, which is a more useful type of energy. The integration of these renewable energy sources with power electronic converters for a variety of applications was made possible by research in this area [1,2]. Concerns about the environment brought on by the production of greenhouse gases by traditional internal combustion (IC) engines have also facilitated the development of electric vehicles (EV). Due to their lack of environmental pollution and innate ability to be quiet, EVs have established a place in the market globally. Initially, these vehicles were used to reduce pollution on golf courses, in warehouses, and within buildings. EVs are often utilised by the elderly and crippled as mobility aids. EVs are currently used for conventional transportation as well. Therefore, using cutting-edge power converter topologies, PV array power is used to charge EV batteries. Lead acid batteries were the first EV battery type, followed by nickel, and most recently lithium cells. Modern electric vehicles (EVs) no longer employ lead acid batteries because of their low chemical leakage, low specific energy, and poor temperature properties. Instead, lithium ion batteries have taken their place. Due to their greater power density, excellent efficiency, small size, and light weight, they are highly favoured. When charging these batteries, the voltage must be precisely controlled. They also feature a large operating temperature range, a long life cycle, and a low self-discharge rate. In addition to these benefits, these batteries have a low danger of exploding if they are unintentionally overcharged or short-circuited. Because of this, lithium ion batteries are best suited for EVs.



In order to charge the battery of an EV, a PV array and a bidirectional DC-DC converter are combined in this work. The bidirectional converter used in the proposed system is operated in boost and buck modes, respectively, in both forward and reverse directions. This makes it easier to power the DC load by forward charging the EV battery from the PV array and reverse charging the EV battery.

2. Operation of the proposed system

According to Fig. 1, the suggested PV-EV battery charger is made up of a solar array, a sepic converter, a half-bridge BIBC, an electric vehicle battery, a backup battery bank, and a controller. To provide a consistent output voltage at the DC link, the controller generates gate pulses for the SEPIC converter. In order to operate BIBC in boost mode to charge the backup battery from the PV array and in buck mode to charge the EV battery from the backup battery, gate pulses to the switches of BIBC are also created. Auxiliary switches Sa, Sb, and Sc receive gate pulses from the controller as well. All of the auxiliary switches are turned on during periods of high solar radiation to connect the dc connection to the EV battery, dc link to the backup battery, and dc link to the PV array via the sepic converter. Switch Sa is switched OFF to isolate the PV array and sepic converter from the dc link when solar irradiation is low. When the solar power is inadequate to charge the backup battery, the switch Sc is set OFF to disconnect the BIBC and the backup battery from the dc link.

The three operating modes of the proposed system—mode 1, mode 2, and mode 3—are described in this section.

2.1 Mode 1 All auxiliary switches are turned ON during peak sunlight hours, when the PV array power generated is at its highest, to charge both the backup battery and the EV battery from the PV array concurrently through a sepic converter and a BIBC, respectively. In order to raise the DC link voltage and charge the backup battery, BIBC functions in the forward direction in this mode.

2.2 Mode 2 PV array output is insufficient to charge an EV battery in low solar irradiation circumstances and during hours when it is not sunny. As a result, the switch Sa is turned off, and switches Sb and Sc are turned on, connecting the EV battery to the backup battery through BIBC. In this mode, the

backup battery voltage is stepped down to allow the electric vehicle battery to be charged.

2.3 Mode 3 Switches Sa and Sb are turned ON and switch Sc is turned OFF to disconnect the BIBC and backup battery bank from the dc link when the electricity provided by the PV array is sufficient to charge only the EV battery.

Converter circuit architecture in the suggested charger

SEPIC converter by regulating its duty ratio with the help of the PI controller, the sepic converter in the suggested charging system provides a consistent output voltage regardless of the PV array voltage. According to Fig. 2, the sepic converter is made up of one IGBT switch, one diode, two inductors, and two capacitors. The sepic converter has two main advantages over buck-boost and cuk converters: (i) it can function in both boost and buck modes depending on the duty ratio; and (ii) it gives the output voltage with the same polarity as the input voltage. The following equation gives the sepic converter's voltage gain:

$$\frac{V_{dc}}{V_{PV}} = \frac{D}{1-D} \quad (1)$$

where D is the duty ratio of the sepic converter, VPV is the voltage of the PV array, and Vdc is the voltage of the DC link. Where VPVmin is the minimum PV array voltage, iPV is the input current ripple, fsw is the switching frequency, and Idc is the dc link, the values of the inductors and capacitors of the sepic converter are selected in accordance with (2) to (4) [17].

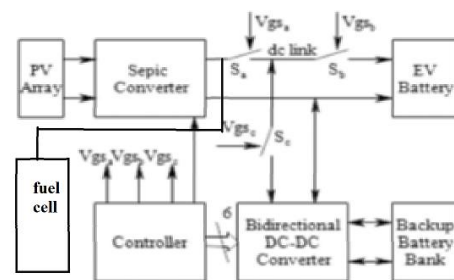


Fig. 1 Block diagram of the EV battery charger



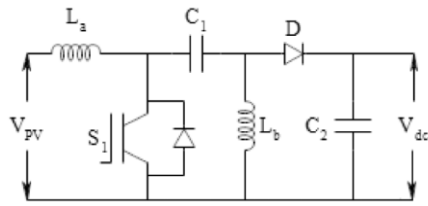


Fig 2. Schematic diagram of sepic converter

D_{max} is the maximum duty ratio computed as follows: current, V_{C1} is the capacitor, C_1 voltage ripple, V_{dc} is the output voltage ripple, and:

$$D_{max} = \frac{V_{dc} + V_D}{V_{PV_{min}} + V_{dc} + V_D} \quad (2)$$

where V_D is the diode voltage drop.

3.2 Bidirectional interleaved DC–DC converter The schematic diagram of the BIDC used in the suggested charging method is shown in Fig. 3. The dc link is on the converter's low voltage side, while the backup battery bank is on its high voltage side. This converter works in boost mode going forward and buck mode going backward. Switches SL_1 , SL_2 , and SL_3 are the active switches in boost mode, whereas switches SU_1 , SU_2 , and SU_3 are the active switches in buck mode. Each switch used in this converter has an antiparallel diode and a parallel snubber capacitor. The inductors L_1 , L_2 , and L_3 function as boost inductors in boost mode whereas, in buck mode, they function as a low-pass filter. The smoothing energy buffer components of this converter are capacitors C_L and C_H . Current ripples are minimised by interleaving inductors. In [20], the operation of a single leg converter is taken into account to analyse the converter's modes of operation. In boost and buck modes, the voltage conversion ratio of the BIDC is determined by equations (6) and (7), respectively.

$$\frac{V_{BackupBatt}}{V_{dc}} = \frac{1}{1 - D_{Boost}} \quad (3)$$

$$\frac{V_{dc}}{V_{BackupBatt}} = D_{Buck} \quad (4)$$

The smoothing energy buffer components of this converter are capacitors C_L and C_H . Current ripples are minimised by interleaving inductors. In [20], the operation of a single leg converter is taken into account to analyse the converter's modes of operation. In boost and buck modes, the voltage conversion ratio of the BIDC is determined by equations (6) and (7), respectively.

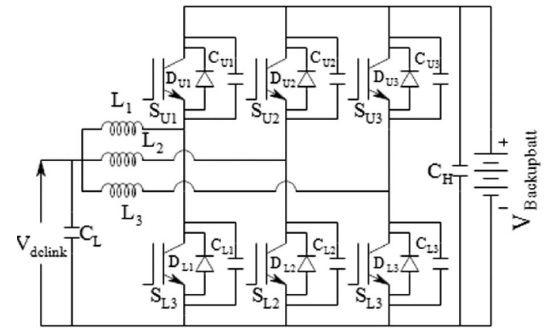


Fig3. Schematic diagram of half-bridge BIDC

3. Design of controller

The proposed charger's controller produces gate pulses for the three auxiliary switches, the BIDC, and the sepicconverter's three switches. Fig. 3 depicts the algorithm used to toggle the auxiliary switches ON and OFF. The PV array voltage and current are sensed by the controller, which also calculates the PV array power. The controller generates gate pulses to turn ON all auxiliary switches in order to charge both the EV battery and the backup battery bank simultaneously from the PV array if the PV array power is greater than the rated power of the EV battery, PR.

The PM, the switch S_c is turned OFF to disconnect the backup battery from the charging system, and switches S_a and S_b are switched ON to charge the EV battery solely from the PV array if the PV array power is less than the rated power of the EV battery but greater than the minimum required power. The switch, S_a , is switched OFF to disconnect the PV array and sepic converter from the charging system if the power of the PV array is less than the minimum needed power, PM. The backup battery may now charge the EV battery because the switches S_b and S_c are both ON. The proposed charging system employs the PI voltage controller to produce gate pulses to the MOSFET in the sepic converter in order to maintain a consistent voltage at the dc link regardless of changes in the PV array voltage. A BIDC consists of three legs, each with two switches. The two switches on the same leg must receive gate pulses that are 180 degrees out of phase with one another. According to the power of the PV array, the controller in the proposed system generates six gate pulses to the BIDC. Gate pulses are generated to the BIDC switches to operate it in boost mode, increasing the dc link voltage to charge the backup battery bank if PV array power exceeds PR. In this mode, the leg 1



switches receive gate pulses with a 0° phase, the leg 2 switches receive gate pulses with a 120° phase shift, and the leg 3 switches receive gate pulses with a 240° phase shift. The gate pulses are generated appropriately to operate BIDC in buck mode, creating a step down voltage at the dc link sufficient to charge the EV battery by the backup battery if the PV array power is less than PM. In this mode, leg 3 switches receive gate pulses with a 0° phase offset, whereas leg 2 and leg 1 switches receive gate pulses that are 120° and 240° phase-shifted from leg 3 switches, respectively.

4. BATTERY

4.1 Energy Storage:

Since electricity is a highly organised form of energy that can be effectively converted into other forms, it has a wider range of applications than other forms of power. It can be turned, for instance, into mechanical form with a near 100% efficiency or into heat with a 100% efficiency. The chaotic nature of heat energy in atoms prevents it from being transformed into electricity with such great efficiency. Because of this, a typical fossil thermal power plant's overall thermal-to-electrical conversion efficiency is under 50%.

Electricity has the drawback of being difficult to store on a large scale. Today, almost all of the electricity utilised is consumed as it is produced. In conventional power plants, where fuel consumption is regularly adjusted to account for load requirements, this presents no difficulty. Due to their intermittent nature, wind and photovoltaic (PV) systems are unable to supply all load demand, 24 hours a day, 365 days a year.

The following broad categories broadly describe the current and upcoming energy storage technologies that could be taken into account for standalone wind or solar power systems:

- Compressed air,
- A flywheel,
- An electrochemical battery,
- A superconducting coil

5. FUEL CELL

An electrochemical device known as a fuel cell uses a fuel source to produce an electrical current. Through reactions between a fuel and an oxidant, started in the presence of an electrolyte, electricity is produced inside a cell. The electrolyte stays inside the cell as the reactants and reaction byproducts flow in and out of it. As long as the essential reactant and oxidant

fluxes are kept up, fuel cells can run constantly. Because reactant is consumed from an external source cells differ from ordinary electrochemical cell batteries because they are a thermodynamically open system. Batteries, on the other hand, function as thermodynamically and must be replenished, fuel closed systems since they chemically store electrical energy.

There are numerous conceivable fuel and oxidant mixtures. A hydrogen fuel cell uses oxygen, typically from the air, as its oxidant and hydrogen as its fuel. Alcohols and hydrocarbons are examples of other fuels. Chlorine and chlorine dioxide are some other oxidants. Although there are many different types of fuel cells, they all function generally the same way. The anode, the electrolyte, and the cathode are the three sandwiched segments that make them up. At the intersections of the three segments, two chemical reactions take place. The combined effect of the two processes is the consumption of fuel, the production of water or carbon dioxide, and the generation of an electrical current that can be utilised to power electrical appliances, commonly referred to as the load.

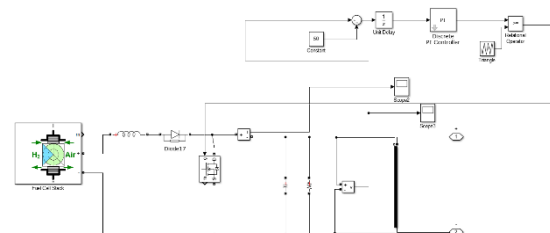


Fig:4 simulation model of fuel cell.

Fuel, often hydrogen, is oxidised at the anode by a catalyst, resulting in the formation of a positively charged ion and a negatively charged electron. The electrolyte is a material created expressly to prevent electrons from passing through while ions can. The electrical current is produced as the liberated electrons move through a wire. To get to the cathode, the ions pass through the electrolyte. When the ions and electrons are once again together at the cathode, they combine with a third substance typically oxygen to produce either water or carbon dioxide. The fuel cells can be connected in series or parallel circuits to deliver the required quantity of energy; series circuits produce higher voltage, and parallel circuits enable larger current to be supplied. A fuel cell stack is one example of such a design. To enable



a greater current from each cell, the cell surface area can be raised.

6. SIMULATION RESULTS AND DISCUSSION

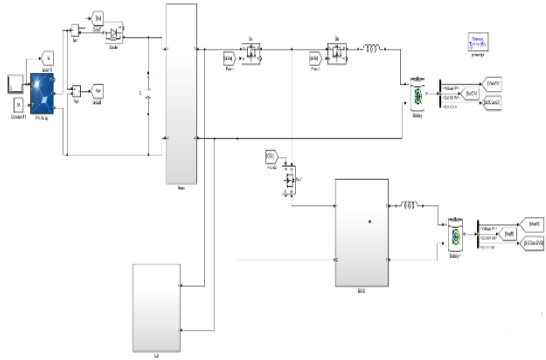


Fig 5. simulation circuit of proposed charger.

The simulation studies of the suggested system employ the MATLAB programme Simulink. The classical equation for the PV array is used to model it [28, 29]. Power MOSFETs, inductors, and capacitors from SimPowerSystemsBlockset in Simulink Library are used to mimic the Sepic and BIDC converter. The Simulink library's PWM generator, pulse generator, logic gates, comparator, multiplier, and PI controller are used to create the controller.

7. Conclusion

In this work, a PV-fuel cell powered off-board EV battery charging system is suggested. This study examines the system's adaptability to continuously charge the EV battery regardless of the irradiation circumstances. The MATLAB software's Simulink environment is used to create and simulate the system. The simulation results highlight the effectiveness of the suggested charger for each of the three modes of operation of the charging system individually.

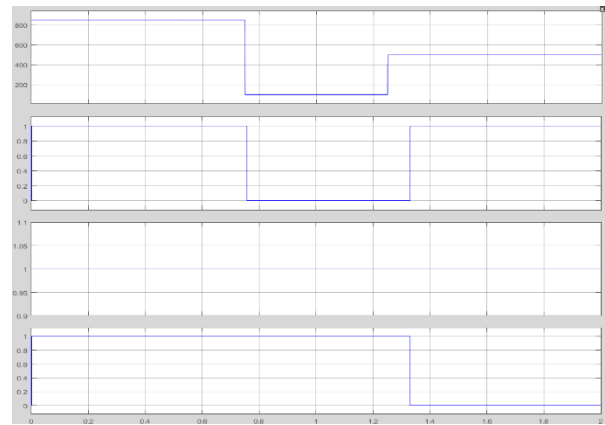


Fig 6. Waveforms of PV array irradiation and gates pulses to the auxiliary switches.

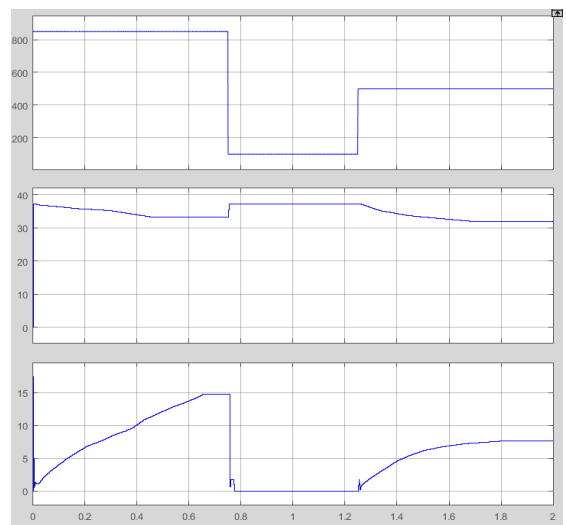


Fig 7a. PV array voltage, V_{pv} & PV array current, I_{pv} .

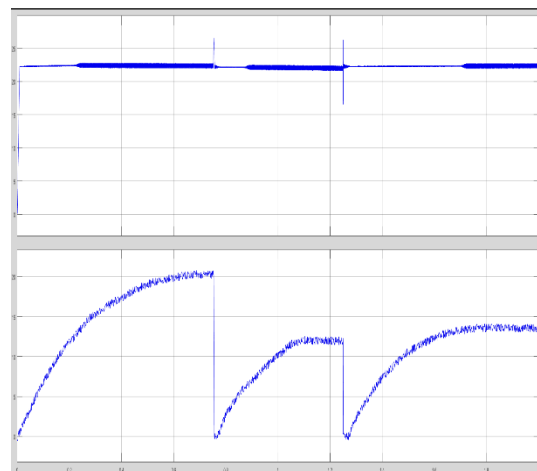


Fig 7b. Dc link voltage, V_{dc} & current, I_{dc} .



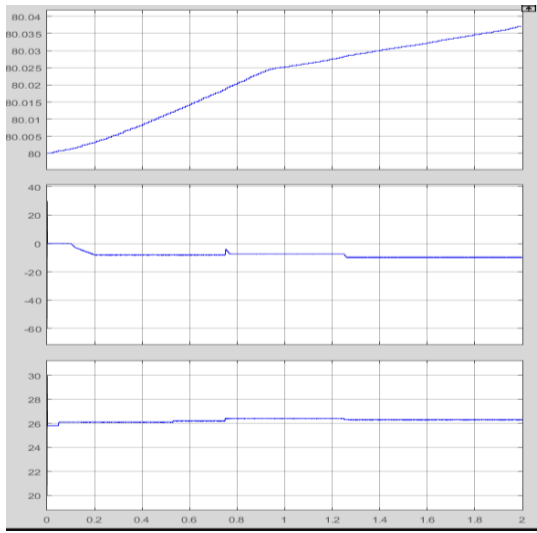


Fig 7c. SOC of EV battery, Ev battery current, I_{batt}& EV battery voltage, V_{batt}.

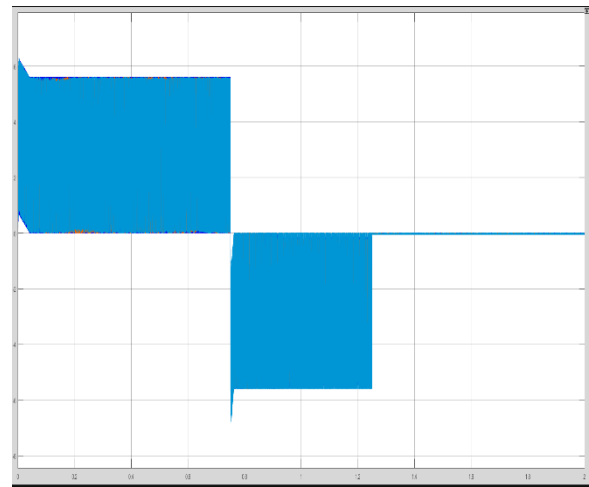


Fig 8a. BIDC currents using fuel cell

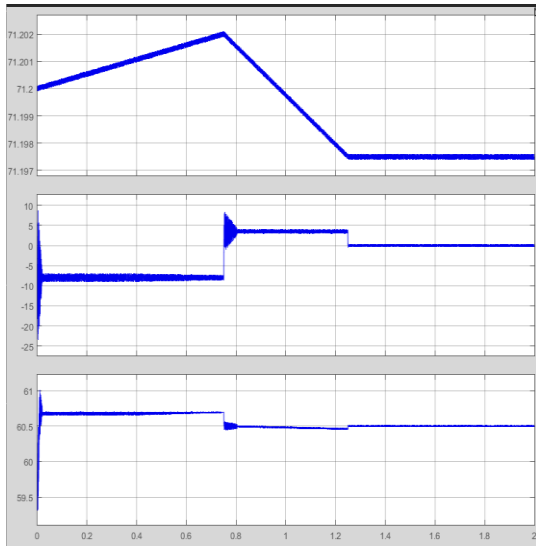


Fig 7d. SOC of backup battery, backup battery current, I_{backup batt}& backup battery voltage, V_{backup batt}.

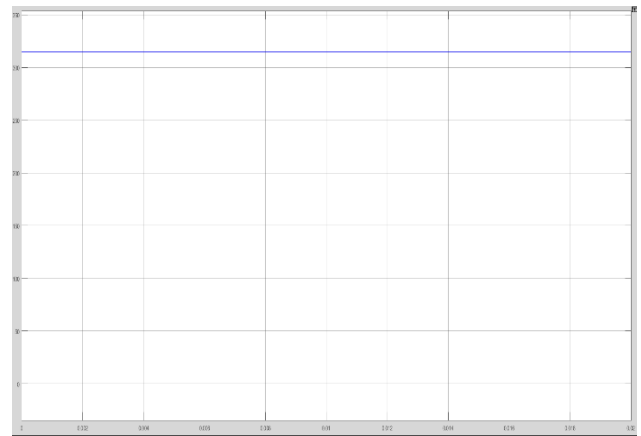


Fig 8b. Fuel cell current

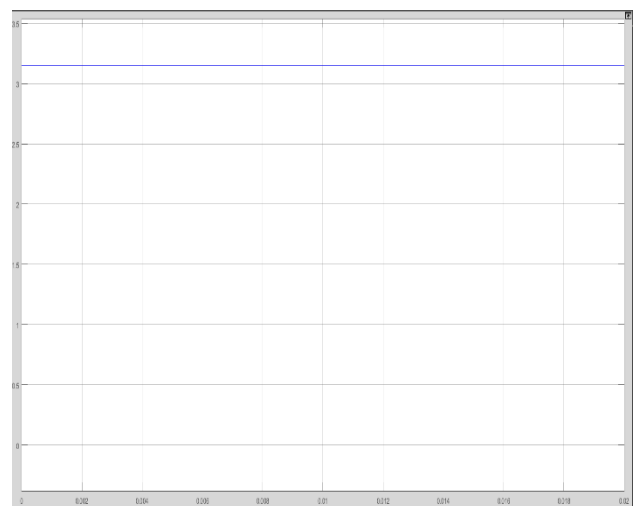


Fig 8c. Fuel cell voltage

The simulation studies of the suggested system employ the MATLAB programme Simulink. The classical equation for the PV array is used to model



it. Power MOSFETs, inductors, and capacitors from SimPowerSystems Blockset in Simulink Library are used to mimic the Sepic and BIBC converter. The Simulink library's PWM generator, pulse generator, logic gates, comparator, multiplier, and PI controller are used to create the controller. The battery models included in the Simulink library are merged with the developed SEPIC converter and BIBC as well as the PV array model to create the suggested charging system as depicted in Fig. 5. Figs. 2 and 3, respectively, illustrate the generated simulation models of the sepic converter and BIBC, which are shown as subsystems. Using the constructed simulation model, the system's dynamic response was examined for PV array irradiation of 850, 100, and 500 W/m² in modes 1, 2, and 3, respectively. Fig. 6 depicts the simulation results, which include the gate pulses to the auxiliary switches as well as the voltage and current waveforms for the PV array. In Fig. 6, radiation waveforms are displayed at a scale of 1 for 1000 W/m². In this method, the EV battery and the backup battery are charged simultaneously. While the gate pulses of the auxiliary switches, V_{gsb} and V_{gsc}, are high and V_{gsa} is low at low irradiation of 100 W/m², respectively, because the PV array's power is insufficient to charge the EV battery. In order to charge the EV battery in this mode, the backup battery bank discharges using BIBC. The auxiliary switches Sa and Sb are turned on during an irradiation of 500 W/m², while switch Sc is turned off, disconnecting the backup battery from the system. Backup battery is segregated and not charged in this mode since PV array power is only adequate for charging EV batteries. In all three modes, the EV battery is continuously charged, as seen in Fig. 6, which also demonstrates that the gate pulses to the switch Sb are always high. In order to prevent trickle charging of the EV battery after it is fully charged, the EV battery is separated from the charging system by activating OFF Switch, Sb. The dynamic waveforms of the PV array, dc link, EV battery, and backup battery are shown in Fig. 7 at the corresponding irradiation values. As seen in Figs. 7a and b, the sepic converter steps down the PV array voltage, V_{pv}, of 33.3 V to the dc link voltage, V_{dc}, of 28 V in mode 1. The EV battery is charging in this mode, as evidenced by the rising state of charge (SOC) and negative current of the battery in Figure 7c. In this mode, the BIBC functions as a boost converter in the forward direction, increasing the dc link voltage from 28 to 60.6 V to charge the backup

battery while increasing SOC, as shown in Fig. 7d. The PV array is isolated in mode 2 (during non-sunny hours and low irradiation circumstances), which causes the PV array voltage, V_{pv}, to rise to its open circuit voltage of 37.25 V and the PV array current, I_{pv}, to be zero amps. These voltage and current waveforms are depicted in Fig. 7a. In order to charge the EV battery during this time, BIBC functions in buck mode in reverse direction, ramping down the backup battery voltage to 27.32 V as illustrated in Fig. 7c. The backup battery is depleted in this mode, as evidenced by the positive current and decline in SOC depicted in Fig. 7d. The backup battery voltage is decreased from 60.6 V to 55.2 V at the conclusion of this mode as depicted in Fig. 7d. Whereas in mode 3, As shown in Figs. 7a and b, the PV array voltage, V_{pv}, of 31.81 V is step down to a dc link voltage, V_{dc}, of 27.6 V to charge the EV battery. Additionally, in this mode, the SOC of the EV battery is rising and the current is negative, signifying that the EV battery is charging. As the backup battery is isolated from the charging system in mode 3, its voltage is kept at 55.2 V and its current is decreased to zero, as illustrated in Fig. 7d. The EV battery's SOC is growing and its current is negative in all three modes, as shown in Fig. 7c, indicating that it receives constant charging from either a PV array or a backup battery.

Fig. 8a depicts the BIBC in each mode of operation. The backup battery discharges in mode 2 as evidenced by the reversal of inductor current flow, and mode 3's zero inductor current indicates that the BIBC is disconnected from the charger.

In parallel support of the solar energy generation, a 50kW and 6255 vdc pemfc fuel cell stack is connected to provide an extra source of power in case solar radiation is disrupted and to provide continuous power supply.

The findings show that the voltage and current parameters are supportive, which charges the backup battery to sustain the EVs battery in the event of a night time application or for numerous EV applications.

The bidc currents are as demonstrated; they are injected by the fuel cell, which raises the soc without draining the backup battery in the case of several EV operations.

8. REFERENCES



[1] Santhosh, T.K., Govindaraju, C.: 'Dual input dual output power converter with one-step-ahead control for hybrid electric vehicle applications', *IET Electr. Syst. Transp.*, 2017, 7, (3), pp. 190–200

[2] Shukla, A., Verma, K., Kumar, R.: 'Voltage-dependent modelling of fast charging electric vehicle load considering battery characteristics', *IET Electr. Syst. Transp.*, 2018, 8, (4), pp. 221–230

[3] Wirasingha, S.G., Emadi, A.: 'Pihef: plug-in hybrid electric factor', *IEEE Trans. Veh. Technol.*, 2011, 60, pp. 1279–1284

[4] Kirthiga, S., Jothi Swaroopan, N.M.: 'Highly reliable inverter topology with a novel soft computing technique to eliminate leakage current in grid-connected transformerless photovoltaic systems', *Comput. Electr. Eng.*, 2018, 68, pp. 192–203

[5] Badawy, M.O., Sozer, Y.: 'Power flow management of a grid tied PV-battery system for electric vehicles charging', *IEEE Trans. Ind. Appl.*, 2017, 53, pp. 1347–1357

[6] Van Der Meer, D., Chandra Mouli, G.R., Morales-EspanaMouli, G., et al.: 'Energy management system with PV power forecast to optimally charge EVs at the workplace', *IEEE Trans. Ind. Inf.*, 2018, 14, pp. 311–320

[7] Xavier, L.S., Cupertino, A.F., Pereira, H.A.: 'Ancillary services provided by photovoltaic inverters: single and three phase control strategies', *Comput. Electr. Eng.*, 2018, 70, pp. 102–121

[10] Farzin, H., Fotuhi-Firuzabad, M., Moeini-Aghaie, M.: 'A practical scheme to involve degradation cost of lithium-ion batteries in vehicle-to-grid applications', *IEEE Trans. Sustain. Energy*, 2016, 7, pp. 1730–1738

[11] Zubair, R., Ibrahim, A., Subhas, M.: 'Multiinput DC–DC converters in renewable energy applications – an overview', *Renew. Sustain. Energy Rev.*, 2015, 41, pp. 521–539

[12] Duong, T., Sajib, C., Yuanfeng, L., et al.: 'Optimized multiport dc/dc converter for vehicle drive trains: topology and design optimization', *Appl. Sci.*, 2018, 1351, pp. 1–17

[13] Santhosh, T.K., Natarajan, K., Govindaraju, C.: 'Synthesis and implementation of a multi-port dc/dc converter for hybrid electric vehicles', *J. Power Electron.*, 2015, 15, (5), pp. 1178–1189

